Received: 22 December 2020 | Revised: 18 February 2021 | Accepted: 3 March 2021

DOI: 10.1111/cas.14874

ORIGINAL ARTICLE

Cancer Science WILEY

RPL34-AS1–induced RPL34 inhibits cervical cancer cell tumorigenesis via the MDM2-P53 pathway

Yuanhang Zhu[1] | Chenchen Ren[1] | Dongyuan Jiang[1] | Li Yang[1] | Yannan Chen[1] | Feiyan Li[1] | Baojin Wang[1] | Yali Zhang[2]

[1]Department of Obstetrics and Gynecology, The Third Affiliated Hospital of Zhengzhou University, Zhengzhou, P.R. China

[2]Department of pathology, Affiliated Tumor Hospital of Zhengzhou University, Zhengzhou, P.R. China

Correspondence
Chenchen Ren, Department of Obstetrics and Gynecology, The Third Affiliated Hospital of Zhengzhou University, No. 7, Front Kangfu Street, Zhengzhou 450052, P.R. China.
Email: renchenchen1106@126.com

Funding information
Key Scientific Research Projects of Higher Education Institutions in Henan Province, Grant/Award Number: 19A320052; Science and Technology Department's Major Program of Henan, China, Grant/Award Number: 161100311100

Abstract

Ribosomal proteins (RPs) are important components of ribosomes and related to the occurrence and development of tumors. However, little is known about the effects of the RP network on cervical cancer (CC). In this study, we screened differentially expressed RPL34 in CC by high-throughput quantitative proteome assay. We found that RPL34 acted as a tumor suppressor and was downregulated in CC and inhibited the proliferation, migration, and invasion abilities of CC cells. Next, we verified that RPL34 regulated the CC through the MDM2-P53 pathway by using Act D medicine, MDM2 inhibitor, and a series of western blotting (WB) assays. Moreover, an antisense lncRNA, RPL34-AS1, regulated the expression of RPL34 and participated in the tumorigenesis of CC. RPL34 can reverse the effect of RPL34-AS1 in CC cells. Finally, by RNA-binding protein immunoprecipitation (RIP) assay we found that eukaryotic initiation factor 4A3 (EIF4A3), which binds to RPL34-AS1, regulated RPL34-AS1 expression in CC. Therefore, our findings indicate that RPL34-AS1–induced RPL34 inhibits CC cell proliferation, invasion, and metastasis through modulation of the MDM2-P53 signaling pathway, which provides a meaningful target for the early diagnosis and treatment of CC.

KEYWORDS
cervical cancer, MDM2, P53, ribosomal protein L34, RPL34-AS1

1 | INTRODUCTION

The discovery of human papillomavirus as the pathogenesis of cervical cancer (CC) has significantly reduced the incidence and mortality of CC.[1] However, according to 2018 global cancer statistics, there were still 570 000 cases (3.2%) and 311 000 deaths (3.3%) of CC worldwide, which ranks as the fourth most frequently diagnosed cancer and the fourth leading cause of cancer death in women.[2] Therefore, in-depth study of the pathogenesis of CC will be expected to further reduce the incidence and mortality by identifying specific molecular markers and effective therapeutic targets.

Ribosomal proteins (RPs) are important components of ribosomes and involved in regulating various biological processes.[3-7] Recent research had found that RPs are also closely related to the occurrence and development

Abbreviations: CC, cervical cancer; HSIL, high-grade intraepithelial lesions; LC-MS/MS, liquid chromatography-mass spectrometry/mass spectrometry; lncRNA, long noncoding RNA; LSIL, low-grade intraepithelial lesions; MDM2, murine double minute gene 2; RIP, RNA-binding protein immunoprecipitation; ROC, receiver operating characteristic; RPs, ribosomal proteins.

of tumors.[8-10] The role of the murine double minute gene 2 (MDM2)-P53 pathway loop in cancers has been widely studied. Activation of P53 stimulates MDM2 expression; conversely, E3 ubiquitin-protein ligase MDM2 mediates p53 constant degradation through a ubiquitin-dependent proteasome pathway.[11,12] Increasing evidence shows that the MDM2-p53 feedback loop can also be regulated by RPs.[9,13-15] RPL34 belongs to the L34E family of RPs, located in the long arm 2 region 5 of human chromosome 4 and contains two exons, encoding 117 amino acids. It is mainly involved in the formation of the 60S subunit. Recent studies have shown that RPL34 is involved in the occurrence and development of malignant tumors, such as glioma, oropharyngeal cancer, esophageal cancer, osteosarcoma, lung cancer and gastric cancer.[16-21] However, the mechanisms and functions of RPL34 are not fully clear in CC. In the present study, we screened and identified RPL34 by proteomics and clarified the detailed mechanism of RPL34-MDM2-P53 in CC.

Antisense long noncoding RNA (lncRNA) transcribed from the antisense strand of a protein-coding gene, often overlapping introns or exons on one or more sense strands, can regulate the transcription and

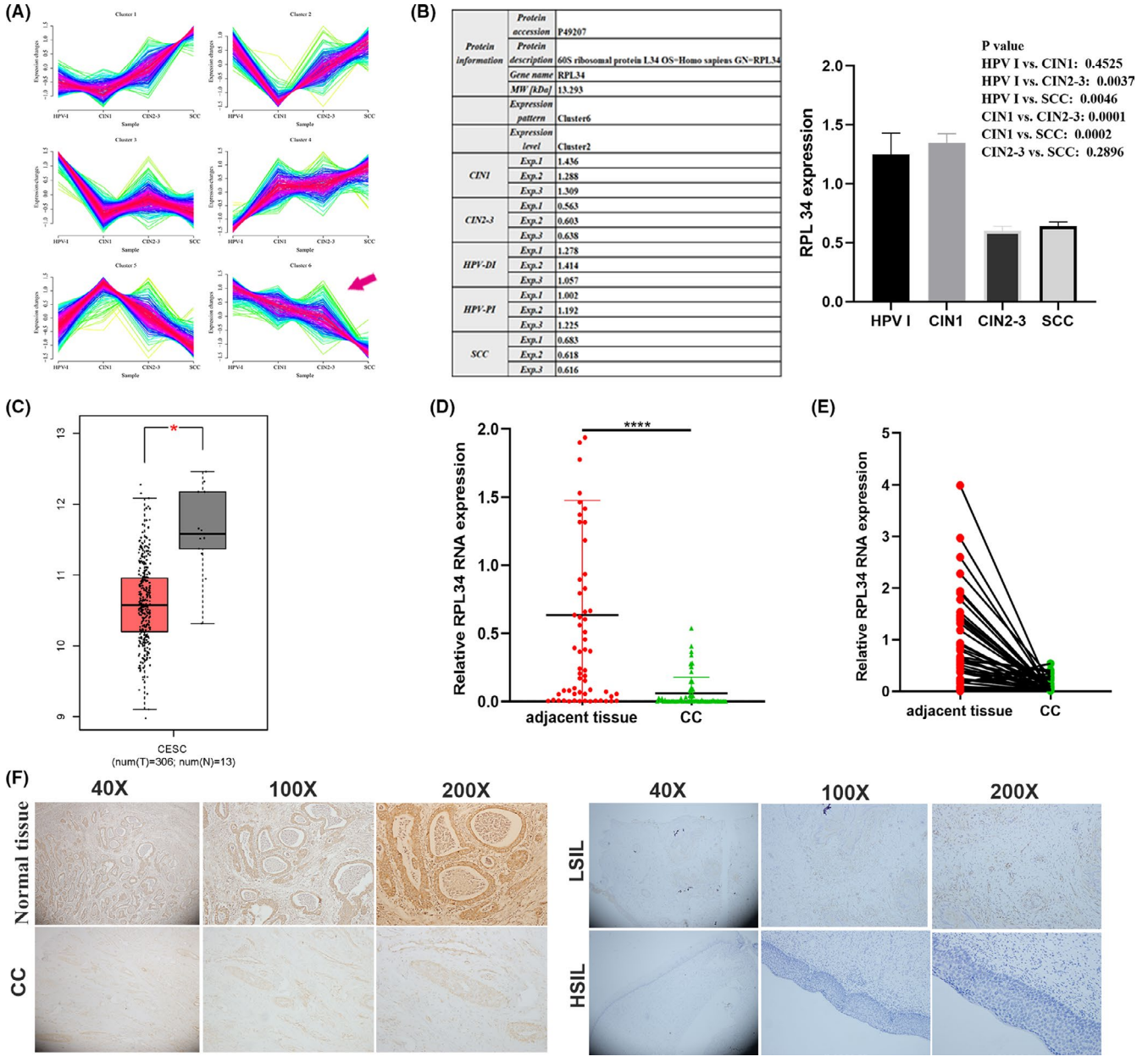

FIGURE 1 Expression of RPL34 in cervical cancer (CC). A, Six protein expression modes in different lesion levels analyzed by proteome assay. The arrow represents protein expression decreases as the severity of cervical lesions increases in cluster 6. B, The expression level and statistical comparison of RPL34 in different cervical lesions. C, The expression levels of RPL34 in CC and normal cervical tissue determined by GEPIA. D and E, The expression level of RPL34 was detected by qRT-PCR in CC tissues and adjacent normal cervical tissues (n = 18); GAPDH served as the internal control. F, the expression of RPL34 was discovered by immunohistochemical staining in normal tissue (n = 32), low-grade intraepithelial lesions (LSIL) (n = 37), high-grade intraepithelial lesions (HSIL) (n = 20), and CC (n = 34), which was presented in three kinds of magnifications (40×, 100×, and 200×). The data are presented as the mean ± SD, $^{*}P < .05$, $^{**}P < .01$, $^{***}P < .001$, $^{****}P < .0001$

antisense of corresponding protein-coding genes.[22-24] RPL34-AS1, as the antisense lncRNA of RPL34, is located head-to-head with RPL34 and may be involved in regulating the function of RPL34. In this study, we designed a series of functional and molecular assays to prove the effect of RPL34-AS1 regulating RPL34 in CC.

2 | MATERIALS AND METHODS

2.1 | Tissue specimens

Tissue specimens used in this study were from patients in The Third Affiliated Hospital of Zhengzhou University between 2016 and 2019. Paraffin specimens included normal cervical tissue (n = 32), low-grade intraepithelial lesions (LSIL) (n = 37), high-grade intraepithelial lesions (HSIL) (n = 20), and CC (n = 34). Fresh tissue specimens for quantitative real-time polymerase chain reaction (qRT-PCR) came from surgery and were fresh frozen in liquid nitrogen, which included CC (n = 93) and paracancer (n = 61). All studies were approved by the Ethics Committee of The Third Affiliated Hospital of Zhengzhou University (2019, Medical Ethics Review No. 46), and informed consent was obtained from all patients.

2.2 | RNA extraction and qRT-PCR

Total RNA was extracted from CC and matched normal tissues, cells, and treated Siha and Hela cells using RNAiso Plus (Cat# 9108; TAKARA BIO INC) according to the manufacturer's protocol. A Hifair II 1st Strand cDNA Synthesis SuperMix kit (Yeasen) was used to synthesize cDNA from RNA according to the manufacturer's protocol. qRT-PCR was performed using a Hieff qPCR SYBR Green Master Mix kit (Yeasen) in an ABI QuantStudio 5 according to the manufacturer's protocol. The mRNA expression levels of genes were measured using the $2^{-\triangle Ct}$ and $2^{-\triangle\triangle Ct}$ method. GAPDH was used as the endogenous control to normalize RNA expression. The primer sequence for qRT-PCR is shown in the Supplementary Material (primer sequence).

2.3 | Cell counting kit-8 (CCK-8) assay

The treated Siha and Hela cells (2×10^3 cells/well) were seeded into a 96-well plate and incubated with complete medium at 37°C for 12, 24, 48, and 72 hours. Then, 10 μL of CCK-8 solution (Dojindo Laboratories) was added into each well. After 3 hours, the absorbance was detected by using a microplate reader at 450 nm.

2.4 | Transwell assays

For migration assay, the treated Siha and Hela cells (1×10^5 cells) in 200 ml of DMEM without FBS were seeded in the upper part of each transwell chamber (pore size, 8 μm; Corning). For the invasion

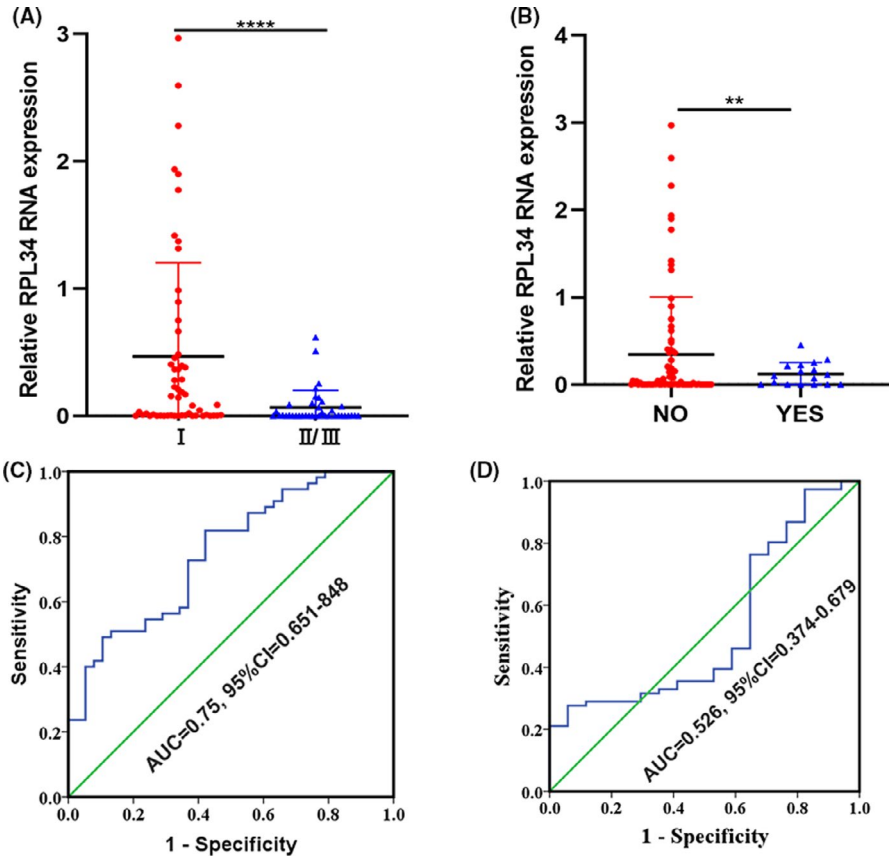

FIGURE 2 The relationship between RPL34 and clinicopathological characteristics in cervical cancer (CC). A, RPL34 expression in clinical staging I was higher than in clinical staging II/III. B, RPL34 expression in patients without lymph node metastasis was higher than in patients with lymph node metastasis. C, The accuracy of RPL34 in diagnosing clinical staging of CC. D, The accuracy of RPL34 in diagnosing lymph node metastasis of CC. The data are presented as the mean ± SD, $^{**}P < .01$, $^{****}P < .0001$

assay, the treated Siha or Hela cells (2×10^5 cells) in 200 ml of DMEM without FBS were seeded in the upper chamber of each insert, which was coated with 50 μL of 2 mg/mL Matrigel growth factor. 650 μL of DMEM with 20% FBS was added to the lower part of the chamber. After 24 hours, the upper chamber of the insert was cleaned, the membranes were fixed with 4% paraformaldehyde (cat. #NO. P1110; Solarbio) for 30 minutes, and stained with 0.1% Crystal Violet Staining Solution (Cat. # G1063; Solarbio) for 15 minutes. The migrated or invasive cells were counted from five random fields using a light microscope.

2.5 | RNA-binding protein immunoprecipitation (RIP) assay

According to the manufacturer's protocol, the RIP assay was performed using a Bersin BIO™ RIP kit (BersinBio) (Catalog bes5101). Hela cells were collected and lysed with RIP lysis buffer. Hela cell lysates (100 μL) were treated with RIP buffer and incubated with Proteinase K and magnetic beads conjugated with anti-EIF4A3(1:30 dilution, Abcam, ab180573) antibody or control (IgG). Next, the immunoprecipitated RNA was extracted. The results were measured by DNA agarose gel electrophoresis and qRT-PCR.

2.6 | Animal studies

Four-week-old female nude mice were purchased from SPF (Beijing) Biotechnology Co., Ltd. The animal studies were approved by the Ethics Committee of The Third Affiliated Hospital of Zhengzhou University(2019, Medical Ethics Review No. 46). In total, 20 mice (n = 5 each group) were injected with stable RPL34 knockdown Hela cells or stable RPL34 overexpression Siha cells resuspended in 100 μL PBS. The animals were sacrificed 28 days after injection, and the tumor volumes were measured every 7 days. The tumor volume was calculated using the following formula: volume (mm^3) = length × $width^2/2$.

2.7 | Statistical analysis

The measurement data were presented as means ± standard deviation (SD) and analyzed using Student's *t* test and ANOVA. The enumeration data were presented as number (percentage, %) and analyzed by chi-square test. Receiver operating characteristic (ROC) curve was used to assess the optimal diagnosis of RPL34. Each experiment was repeated at least three times. Two-sided *P*-value less than .05 was considered statistically significant. All statistical analyses were performed with SPSS 24 statistical software (IBM Corporation) and GraphPad Prism 8.02.

Additional methods are described in the Supplementary Material (supplementary methods).

3 | RESULTS

3.1 | Identification of RPL34 in CC via proteomics analysis

We determine the expression status of proteins in different levels of cervical lesions through liquid chromatography-mass spectrometry/mass spectrometry (LC-MS/MS) analysis. The proteins in cluster 4 and cluster 6 were positively/negatively correlated with the severity of cervical lesion (Figure 1A). 247 proteins belong to cluster 6, and three of these are RPs: RPL34, RPL35, and RPL6 (Figure 1B; Document S1). We then evaluated the expression of RPs in CC and normal cervical tissue with the online TCGA-based tool GEPIA.[25] Only RPL34 differentially expressed by GEPIA was determined (Figure 1C). We then validated RPL34 on tissue specimens. qRT-PCR assay revealed that the expression level of RPL34 was significantly decreased in CC tissues compared with that in paracancerous tissues (n = 61, $P < .0001$, Figure 1D,E), while there was no significant difference in the expression of RPL34 between cervical squamous cell carcinoma and adenocarcinoma ($P = .587$). Immunohistochemistry assay revealed that the positive intensity of RPL34 in CC is lower than in normal cervical tissue, LSIL and HISL, but the positive intensity for cervical gland tissue is higher than for epithelial tissue (Figure 1F).

TABLE 1 The relationship between RPL34 expression and clinicopathologic features of cervical cancer

Clinicopathologic feature	N (%)	RPL34 (mean ± SE)	*P*-value
Age			
<40	20 (21.51)	0.58 ± 0.20	.109
≥40	73 (78.49)	0.23 ± 0.06	
Histology			
Squamous cell cancer	59 (63.44)	0.34 ± 0.08	.775
Adenocarcinoma	27 (29.03)	0.26 ± 0.11	
Others	7 (7.53)	0.20 ± 0.13	
Clinical staging			
I	55 (59.14)	0.47 ± 0.10	.000
II/III	38 (40.86)	0.07 ± 0.02	
Differentiation			
Well to moderate	58 (62.37)	0.27 ± 0.08	.539
Poor	35 (37.63)	0.35 ± 0.11	
Lymphatic vascular space invasion			
No	76 (81.72)	0.30 ± 0.07	.852
Yes	17 (18.28)	0.33 ± 0.16	
Lymph node metastasis			
Negative	76 (81.72)	0.34 ± 0.08	.008
Positive	17 (18.28)	0.12 ± 0.03	

3.2 | RPL34 was correlated with clinicopathological characteristics of CC

Ninety-three fresh CC tissues were used to detect RPL34 expression by qRT-PCR analysis. Results showed that histology type, differentiation degree, and lymphatic vascular space invasion of patients have little effect on RPL34 expression. However, RPL34 expression was correlated with the clinical stage and the lymph node metastasis (Figure 2A,B; Table 1). Next, we used the ROC curve to further calculate the optimal threshold for RPL34 to diagnose clinical staging II/III and lymph node metastasis. The results confirmed the diagnostic value of RPL34 for clinical staging but not lymph node metastasis; the optimal threshold was 0.397, and at this time the sensitivity was 80.0% and the specificity 57.9% (Figure 2C,D).

3.3 | RPL34 was associated with proliferation, migration, and invasion in CC cells

First, we detected the expression of RPL34 in normal human cervical epithelial cells (HCerEpiC) and CC cells (Hela, Siha, C33a, and Caski). We found that RPL34 was highly expressed in C33a and Hela cells but relatively poorly expressed in Siha cells (Figure 3A). After searching in the IARC TP53 Database (https://p53.iarc.fr/

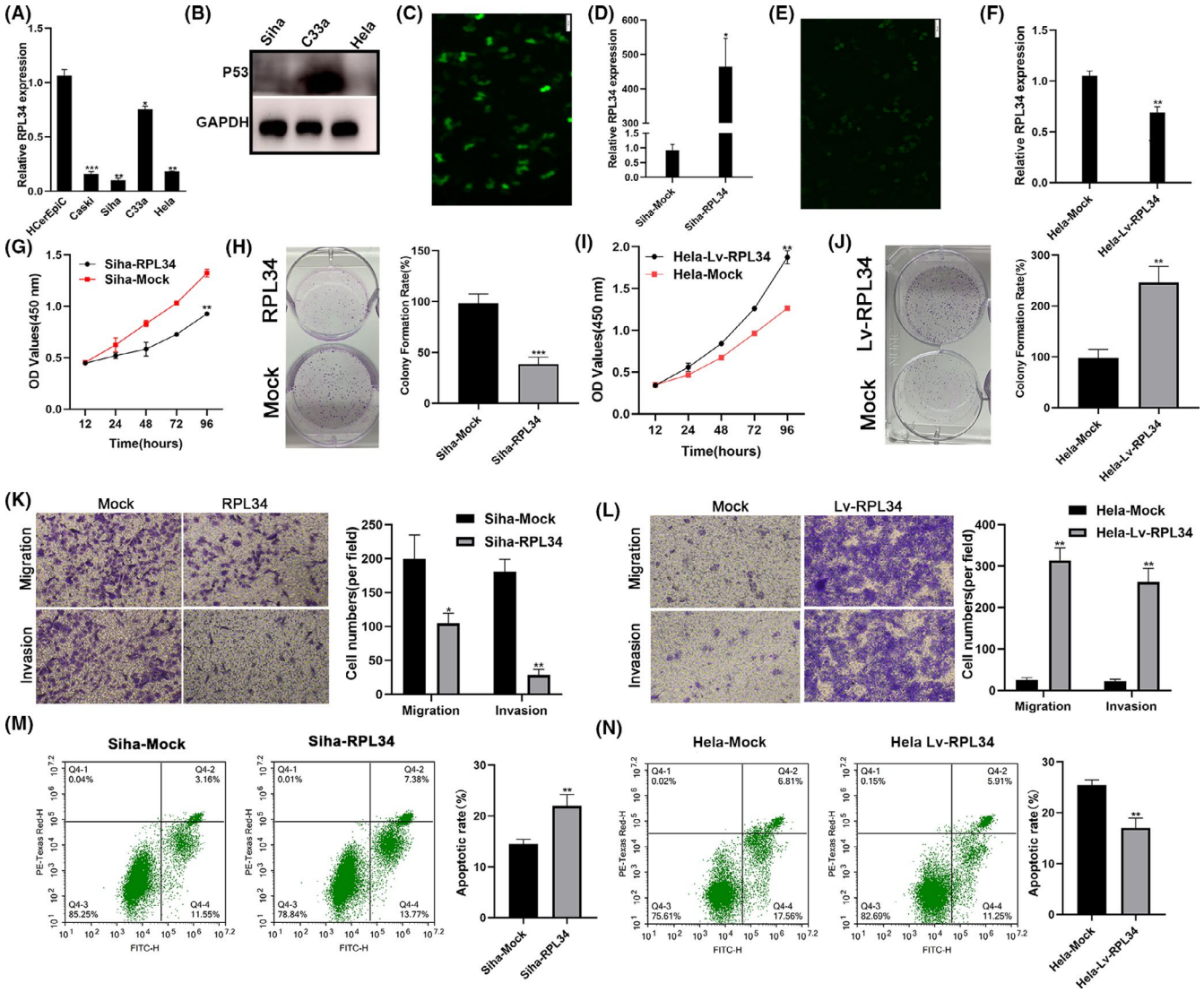

FIGURE 3 RPL34 suppresses the proliferation, migration, and invasion of cervical cancer (CC) cells. A, RPL34 expression was analyzed by qRT-PCR in normal human cervical epithelial cells (HCerEpiC) and CC cells (Hela, Siha, C33a, and Caski). B, WB assay detected the RPL34 protein expression in Hela, Siha, and C33a cells. C, Immunofluorescence showed that RPL34 overexpression and mock plasmid were transfected into Siha cells, proved by the appearance of green fluorescent protein. D, qRT-PCR was performed to detect RPL34 expression in treated Siha cells. E, Immunofluorescence showed the RPL34 interference lentivirus and mock were transfected into Hela cells, proved by the appearance of green fluorescent protein. F, qRT-PCR was performed to detect RPL34 expression in treated Hela cells. G-J, Cell proliferation abilities were detected by CCK-8 and colony formation assays in transfected Siha and Hela cells. K and L, Cell migration and invasion abilities were measured with Transwell assays. M and N, Flow cytometry was used to detect apoptosis. The data are presented as the mean ± SD, $^{*}P < .05$, $^{**}P < .01$, $^{***}P < .001$

Scope.aspx) and verification via WB assay (Figure 3B), we chose Hela and Siha cells for further study due to their wild type of P53. Next, Siha cells were transfected with RPL34 or mock plasmids, and qRT-PCR was used to detect the transfection efficiency. The results indicated that the RPL34 overexpression vector was efficient ($P = .0102$, Figure 3C,D). Simultaneously, RPL34 was successfully knocked down in Hela cells ($P = .0083$, Figure 3E,F). Furthermore, we confirmed that overexpression of RPL34 significantly inhibited the proliferation ability of Siha cells ($P = .0063$, Figure 3G and $P = .0009$, Figure 3H). Silencing of RPL34 significantly promoted the proliferation ability of Hela cells ($P = .0053$, Figure 3I and $P = .0021$, Figure 3J). Next, we observed that overexpression of RPL34 significantly inhibited the migration and invasion abilities of Siha cells ($P = .0124$, $P = .002$, Figure 3K). Silencing of RPL34 significantly promoted the migration and invasion abilities of Hela cells ($P = .0042$, $P = .0052$, Figure 3L). Furthermore, flow cytometry assay revealed that RPL34 promoted the apoptosis of CC cells ($P = .0062$, $P = .0029$, Figure 3M,N).

3.4 | RPL34 inhibited the proliferation, migration, and invasion via MDM2-P53

Proteins in cluster 4 and cluster 6 were mainly associated with complement and coagulation cascades, vesicle-mediated transport, ubiquitin-mediated proteolysis, and ribosome (Figure 4A; Document S2). We could also see that RPL34 interacted with many RPs (Figure 4B). Studies have shown that RPs are widely involved in the MDM2-P53 pathway to regulate the occurrence and development of cancer.[15] Therefore, we speculate that RPL34 participates in the regulation of CC through MDM2-P53. Results illustrated that when RPL34 was overexpressed, the expression of P53 protein increased, and when RPL34 was silenced,

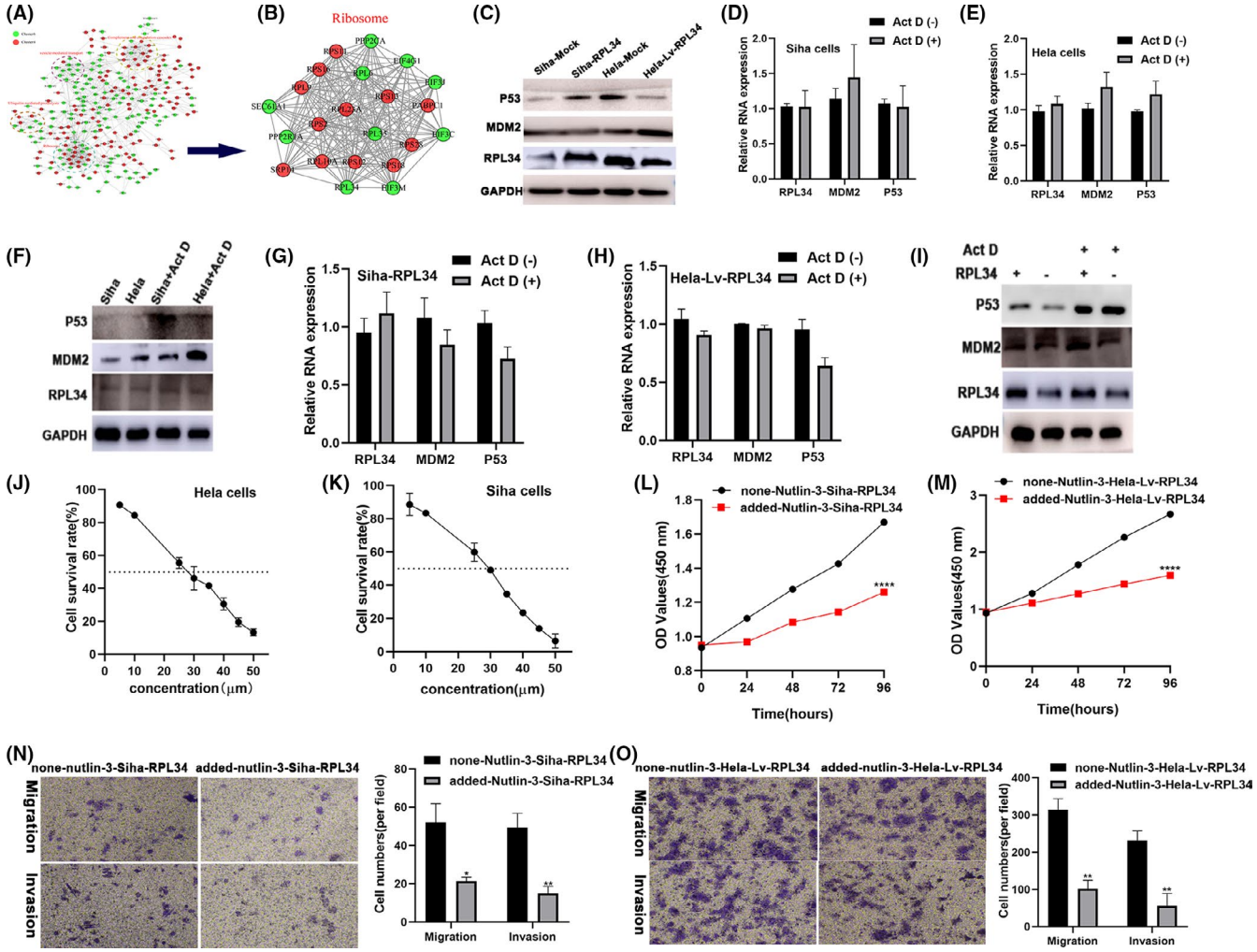

FIGURE 4 RPL34 inhibited the proliferation, migration, and invasion via the MDM2-P53 pathway. A and B, Protein-protein interactions analysis revealed the function of RPL34. C, WB assay detected the RPL34 protein expression in treated Siha and Hela cells. D-F, qRT-PCR and WB assay analyzed the RPL34 expression after added Act D (5 nmol/L) in Hela and Siha cells. G-I, qRT-PCR and WB assay analyzed RPL34 expression after added Act D (5 nmol/L) in transfected Hela and Siha cells. J and K, The half-maximal inhibitory concentration (IC50) for Siha and Hela cells with Nutlin-3 added. L and M, Cell proliferation abilities were detected by CCK-8 in transfected Siha and Hela cells with or without Nutlin-3. N and O, Cell migration and invasion abilities were measured with Transwell assays in transfected Siha and Hela cells with or without Nutlin-3. The data are presented as the mean ± SD, $^{*}P < .05$, $^{**}P < .01$, $^{****}P < .0001$

the expression of P53 decreased (Figure 4C). It has been previously demonstrated that low doses of actinomycin D (Act D) (5 nmol/L) exclusively inhibits RNA polymerase I–driven transcription and induces ribosomal stress.[26] Treating Siha or Hela cells with 5 nmol/L Act D did not affect the level of RPL34 on both RNA and protein level but clearly increased the expression of MDM2 and p53 not on RNA level but on protein level (Figure 4D-F). Weirdly, when silencing or overexpressing RPL34 combined with Act D, the expression level of RNA in MDM2 and p53 was unchanged, while the protein level increased; moreover, this increasing was stronger than in the case of Act D alone. (Figure 4G-I). To further certify the relationship between RPL34 and MDM2/P53, we added MDM2 inhibitor (Nutlin-3) to the cell culture medium of Siha-RPL34 or Hela-Lv-RPL34. First, we used Siha cells and Hela cells to find the optimum action concentration for Nutlin-3. We found that the half-maximal inhibitory concentration (IC50) for Siha cells and Hela cells was about 30 μmol/L after 6 hours (Figure 4J,K). Next, CCK8 assay revealed that the proliferation ability of the added Nutlin-3's Siha-RPL34 cells and the added Nutlin-3's Hela-Lv-RPL34 cells decreased ($P < .0001$, $P < .0001$, Figure 4L,M). Similarly, the ability of migration and invasion for the added Nutlin-3's Siha-RPL34 cells and the added Nutlin-3's Hela-Lv-RPL34 cells decreased ($P = .0327$ and $P = .0093$, $P = .0039$ and $P = .0099$, Figure 4N,O). This means that MDM2 inhibitor Nutlin-3 could reverse the effects of RPL34 knockdown.

3.5 | RPL34-AS1 regulated the expression of RPL34 and was involved in the tumorigenesis in CC

We explored that RPL34-AS1 acts as an antisense transcript of RPL34 (Figure 5A). The expression of different transcripts

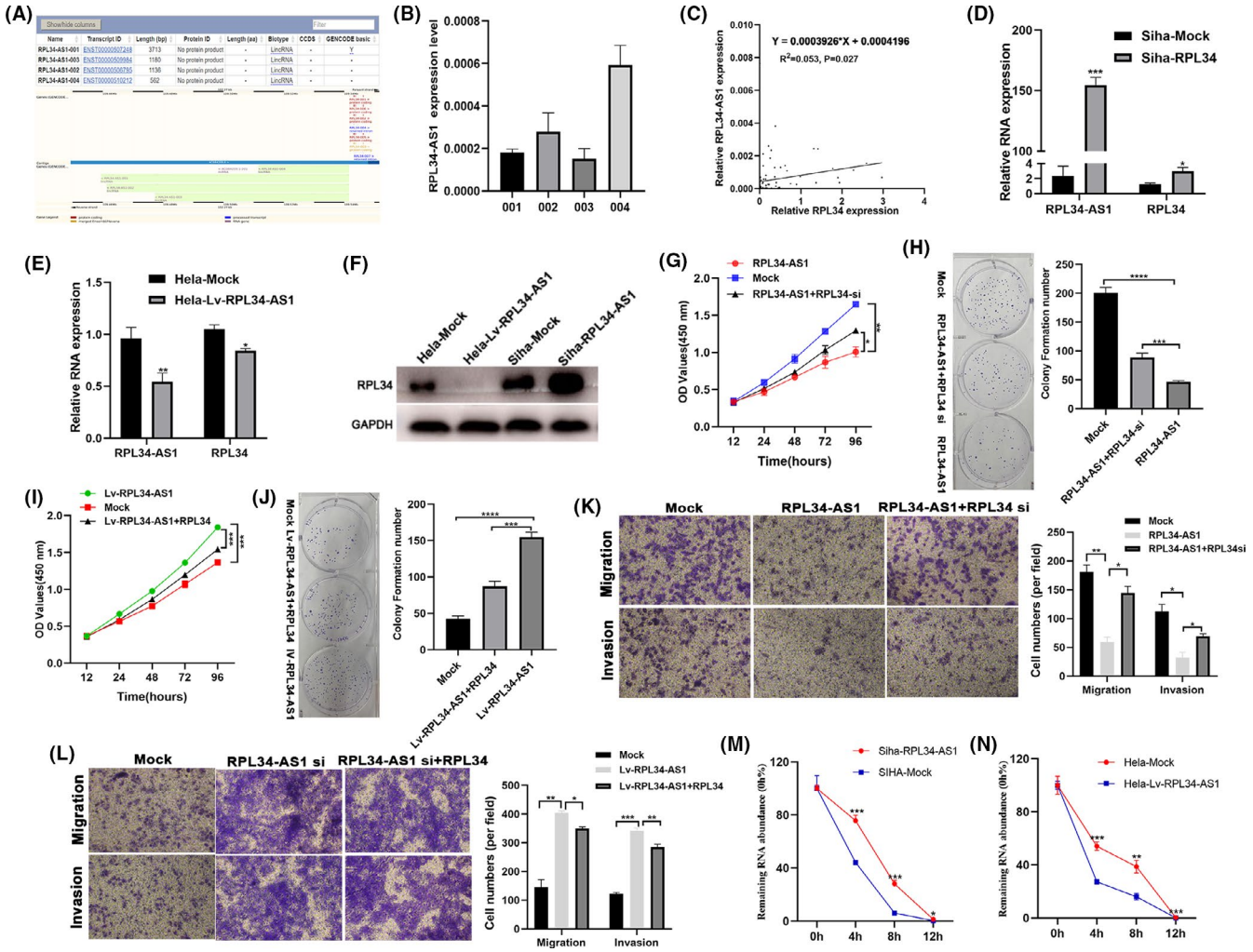

FIGURE 5 RPL34-AS1 regulated the expression of RPL34 in cervical cancer (CC). A, Characterization of RPL34-AS1 in human genome. B, qRT-RCR detected the expression of four RPL34-AS1 transcripts. C, Correlation between the expression of RPL34-AS1 and RPL34 was evaluated by Pearson's correlation test ($r^2 = .053$, $P = .027$). D and E, qRT-RCR detected the expression of RPL34-AS1 and RPL34 in RPL34-AS1–overexpressing (Siha) or –silencing (Hela) cells. F, The protein expression levels of RPL34 were measured by Western blot assays in treated Siha and Hela cells. G-J, CCK-8 and colony formation assays were performed to assess the proliferation ability of the transfected Siha and Hela cells. K and L, Cell migration and invasion abilities were measured with transwell assays in transfected Siha and Hela cells. M and N, qRT-RCR detected the expression of RPL34 0, 4, 8, and 12 h after adding Act D (5 μg/mL). The data are presented as the mean ± SD, $^*P < .05$, $^{**}P < .01$, $^{***}P < .001$, $^{****}P < .0001$

of RPL34-AS1in Siha cells is shown in Figure 5B. We chose the RPL34-AS1-002 version for research based on previous studies in other cancers.[27,28] qRT-PCR assay revealed that the expression of RPL34-AS1 is positively related to the expression of RPL34 in CC (Figure 5C). Next, Siha cells were transfected with RPL34-AS1 or mock plasmids and Hela cells were transfected with lentivirus that knocked down RPL34-AS1 or mock plasmids. Results suggested that RPL34 expression increased after overexpressing RPL34-AS1 (P = .0004, P = .0121, Figure 5D,F) and decreased after silencing RPL34-AS1 (P = .0012, P = .0241, Figure 5E,F). More importantly, we found that RPL34-AS1 suppressed Siha cell proliferation, and silencing of RPL34 attenuated this suppression (P = .0027, P = .0318, Figure 5G; P < .0001, P = .0008, Figure 5H). On the other hand, silencing of RPL34-AS1 accelerated Hela cell proliferation, and RPL34 weakened this acceleration (P = .0009, P = .0008, Figure 5I; P < .0001, P = .0003, Figure 5J). Furthermore, we found that RPL34-AS1 suppressed Siha cell migration and invasion, and silencing of RPL34-AS1 attenuated this suppression (P = .0046, P = .0172, and P = .0166, P = .028, Figure 5K). On the other hand, silencing of RPL34-AS1 accelerated Hela cell migration and invasion, and RPL34 weakened this acceleration (P = .0018, P = .0129, and P = .0009, P = .0094, Figure 5L) Studies have reported that antisense lncRNA can regulate the stability of the RNA encoded by the sense strand.[23] Thus, we used a large dose of Act D (5 μg/mL) to test RNA stability after overexpressing or silencing RPL34-AS1, and the results showed that RPL34-AS1 can stabilize RPL34 (Figure 5M,N).

3.6 | EIF4A3 regulated the expression of RPL34-AS1 in CC

Using bioinformatics analysis software (starBase),[29] we found that there are three binding sites for EIF4A3 which are present in the upstream of RPL34-AS1 (named a, b, c; Figure 6A,B). First, we used the EIF4A3 antibody to perform RIP experiments, and the results showed that EIF4A3 could bind to the site of a, b, c, and RPL34 (Figure 6C). Then, we knocked down EIF4A3 using siRNA (P = .0284 [si 01], P = .041 [si 03]; Figure 6D) and found that the expression of RPL34-AS1 was significantly reduced (P = .031[si 01], P = .0388[si 03]; Figure 6E). At the same time, after transfecting the plasmid with overexpression of EIF4A3, EIF4A3 (P < .0001, Figure 6F) and RPL34-AS1 expression increased (P = .0031, Figure 6G).

3.7 | RPL34 enhances CC growth in vivo

Stable transfected Hela and Siha cells (100 μL, 5 × 10^6 cells per mouse) were injected in nude mice, and tumors were allowed

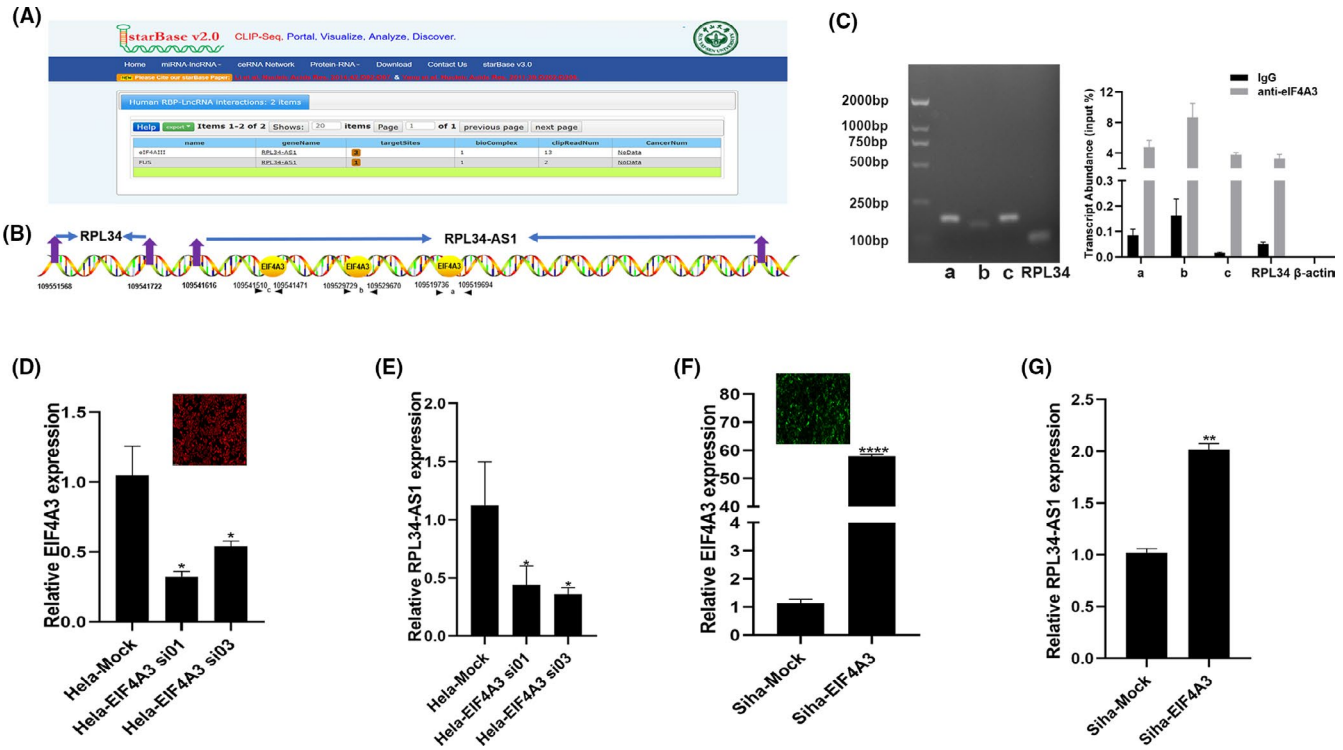

FIGURE 6 EIF4A3 regulates RPL34-AS1 expression. A and B, The binding sites of EIF4A3 were predicted in RPL34-AS1 transcript using starBase. C, qRT-PCR was used to detect the transcript abundance relative to input. D and E, Hela cells were transfected with control or EIF4A3 siRNA, and expression of EIF4A3 and RPL34-AS1 was detected by qRT-PCR. F and G, Siha cells were transfected with control or EIF4A3 overexpressing plasmid, and expression of EIF4A3 and RPL34-AS1 was detected by qRT-PCR. The data are presented as the mean ± SD, *P < .05, **P < .01, ****P < .0001

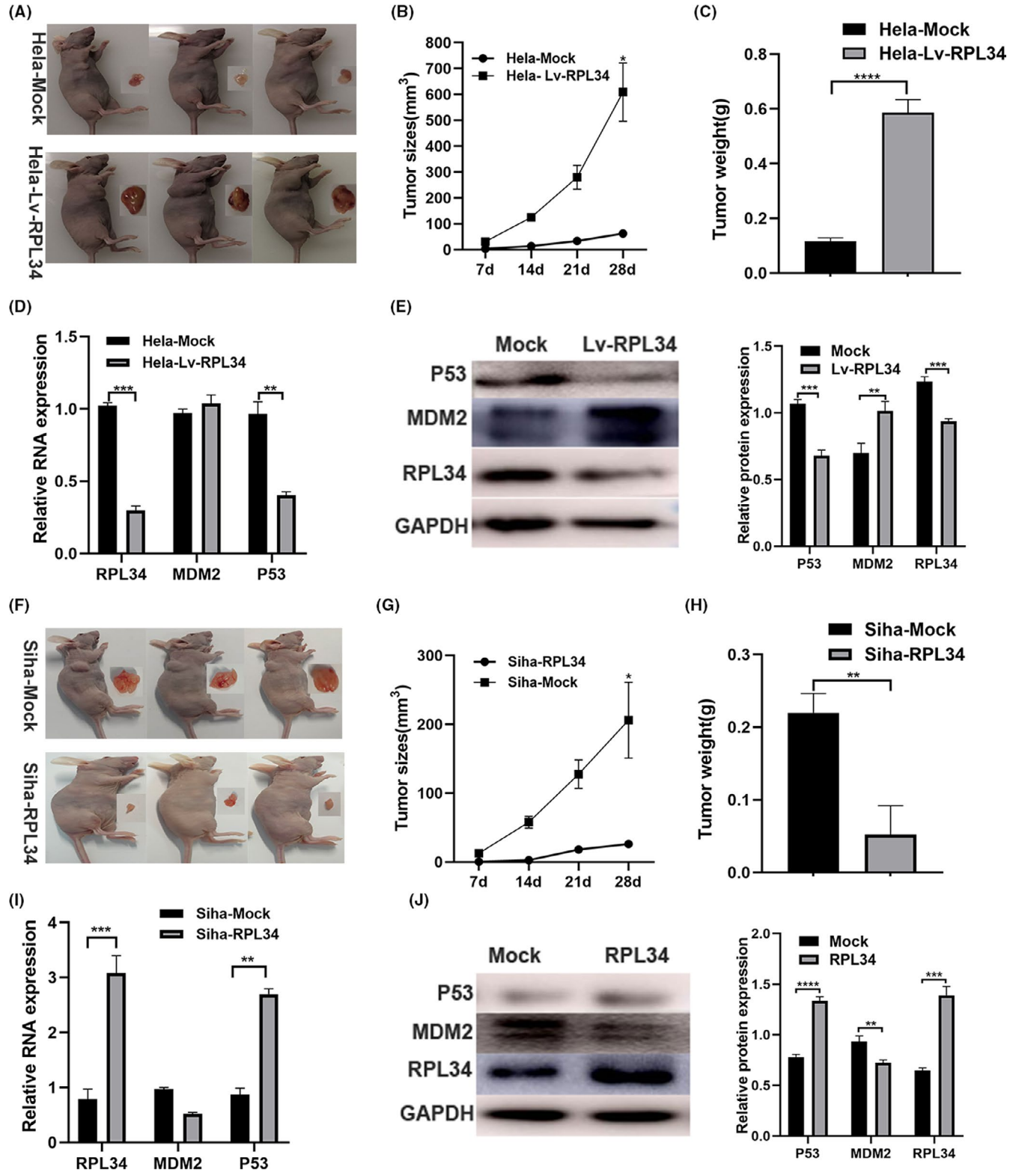

FIGURE 7 RPL34 inhibited cervical cell (CC) growth in vivo. A and C, The stable RPL34-mock and RPL34-Lv Hela cells (5×10^6 cells) were injected into nude mice, and tumors were allowed to develop for 7, 14, 21, and 28 d. The tumor size at 28 d is presented, and the tumor size and weight were determined. D, The expression of RPL34, MDM2, and P53 were evaluated by qRT-PCR assay. E, WB assay was used to detect the expression of RPL34, MDM2, and P53, and the proteins were quantified by image J. F-H, The stable mock and RPL3-overexpressing Siha cells (5×10^6 cells) were injected into nude mice, and tumors were allowed to develop for 7, 14, 21, and 28 d. The tumor size at 28 d is presented, and the tumor size and weight were determined. I, The expression of RPL34, MDM2, and P53 were evaluated by qRT-PCR assay. J, WB assay was used to detected the expression of RPL34, MDM2, and P53, and the proteins were quantified by image J. The data are presented as the mean ± SD, $^*P < .05$, $^{**}P < .01$, $^{***}P < .001$, $^{****}P < .0001$

to grow for 7, 14, 21, and 28 days. The results indicated that silencing of RPL34 generated an outstanding increase in the rate of xenograft subcutaneous tumor growth ($P = .0277$, $P < .0001$, Figure 7A-C), while overexpression of RPL34 decreased the tumor growth ($P = .0321$, $P = .0037$, Figure 7F-H). qRT-PCR assay showed that silencing of RPL34 downregulated P53 expression ($P = .0001$, $P = .1519$, $P = .0037$, Figure 7D), and overexpression of RPL34 upregulated P53 expression ($P = .0001$, $P = .1229$, $P = .0037$, Figure 7I). Western blotting assay data showed that silencing of RPL34 upregulated MDM2 expression, while the P53 expression decreased ($P = .003$, $P = .0057$, $P = .0002$, Figure 7E); however, overexpression of RPL34 downregulated MDM2 expression, while the expression of P53 increased ($P < .0001$, $P = .0042$, $P = .0002$, Figure 7J).

4 | DISCUSSION

Clinical data show that the prognosis of early CC is generally better in patients with surgery, while with the increase of tumor volume and the appearance of metastasis, poor prognosis occurrs despite suffering surgery, radiotherapy, or chemotherapy.[30] Therefore, it is particularly indispensable to explore the mechanism of proliferation and metastasis in CC. In the present study, we explored the protein expression in cervical exfoliated cells of patients with different cervical lesions and found RPL34, which decreases as the severity of cervical lesions increases. qRT-PCR confirms that RPL34 mRNA level is lower in CC than in normal tissue. In vivo and in vitro experiments have also confirmed that RPL34 inhibits proliferation, invasion, and metastasis of CC. These results further support that RPL34 acts as a tumor suppressor in CC, which is different from other cancers in which RPL34 expression is higher in cancer tissue than in matched normal tissue.[16-21] Additionally, we found that the expression of MDM2 increased and P53 decreased when RPL34 expression decreased; however, the expression of MDM2 decreased and P53 increased when RPL34 expression increased both in vivo and in vitro, which indicates that RPL34 may be a new composition in RPs -MDM2-P53 system. At the same time, after altering the expression of RPL34, MDM2 and P53 expression in Act D was higher than in Act D without altered expression of RPL34, which supports that RPL34 is involved in the regulation of the MDM-P53 pathway. Furthermore, the MDM2 inhibitor weakens the effects of RPL34 knockdown, which also indicates that RPL34 inhibits the occurrence of CC through the MDM2-P53 pathway. This discovery provides a theoretical basis for the application of MDM2 inhibitors in the targeted treatment of CC.

Previous research has indicated that antisense lncRNA participates in the occurrence and development of cancer by regulating the sense strand coding RNA.[24,31,32] In this study, we found that lncRNA RPL34-AS1 regulates RPL34 expression, and RPL34 can make up for the effect of RPL34-AS1 on proliferation, invasion, and metastasis of CC cells. The possible mechanism involved is regulating the stability of RPL34 mRNA. Therefore, we concluded that RPL34-AS1 is involved in the development of CC by regulating RPL34. Of course, further evidence is required to conclude how RPL34-AS1 regulates the expression of RPL34. lncRNAs have been reported to regulate gene expression post-transcriptionally through interacting with RNA-binding proteins (RBPs).[33,34] EIF4A3 is an important component of the exon junction complex (EJC), which is involved in splicing and polyadenylation, as well as mRNA export and mRNA localization.[35] In this study, we found that EIF4A3 could bind to the region of RPL34-AS1 and regulate its expression. Synthetically, we concluded that EIF4A3 can induce RPL34-AS1 transcription.

In conclusion, our study showed that RPL34 acts as a tumor suppressor and inhibits CC proliferation, migration, and invasion. The mechanism may be through the MDM2-P53 pathway, and a kind of antisense lncRNA, RPL34-AS1, regulates its expression. Therefore, our research provides a solid basis for the elucidation of the mechanism of CC and a meaningful target for its early diagnosis and treatment.

ACKNOWLEDGMENTS

This work was supported by the Key Scientific Research Projects of Higher Education Institutions in Henan Province (no. 19A320052); the Science and Technology Department's Major Program of Henan, China (no. 161100311100).

CONFLICT OF INTEREST

The authors have no commercial or other associations that might pose a conflict of interest.

ETHICS APPROVAL AND CONSENT TO PARTICIPATE

The present study was approved by The Third Affiliated Hospital of Zhengzhou University.

CONSENT FOR PUBLICATION

Not applicable.

DATA AVAILABILITY STATEMENT

The datasets analyzed during the current study are available from the corresponding author on reasonable request.

ORCID

Chenchen Ren https://orcid.org/0000-0003-3308-2447

REFERENCES

1. Wentzensen N, Arbyn M. HPV-based cervical cancer screening-facts, fiction, and misperceptions. *Prev Med*. 2017;98:33-35.
2. Ferlay J, Colombet M, Soerjomataram I, et al. Estimating the global cancer incidence and mortality in 2018: GLOBOCAN sources and methods. *Int J Cancer*. 2019;144:1941-1953.
3. Rao S, Peri S, Hoffmann J, et al. RPL22L1 induction in colorectal cancer is associated with poor prognosis and 5-FU resistance. *PLoS ONE*. 2019;14:e0222392.
4. Wang W, Nag S, Zhang XU, et al. Ribosomal proteins and human diseases: pathogenesis, molecular mechanisms, and therapeutic implications. *Med Res Rev*. 2015;35:225-285.

5. Seong KM, Jung S-O, Kim HD, et al. Yeast ribosomal protein S3 possesses a β-lyase activity on damaged DNA. *FEBS Lett*. 2012;586:356-361.
6. Kim Y, Kim HD, Kim J. Cytoplasmic ribosomal protein S3 (rpS3) plays a pivotal role in mitochondrial DNA damage surveillance. *Biochim Biophys Acta*. 2013;1833:2943-2952.
7. Sen N, Paul B, Gadalla M, et al. Hydrogen sulfide-linked sulfhydration of NF-κB mediates its antiapoptotic actions. *Mol Cell*. 2012;45(1):13-24.
8. Dong Z, Jiang H, Liang S, Wang Y, Jiang W, Zhu C. Ribosomal protein L15 is involved in colon carcinogenesis. *Int J Med Sci*. 2019;16:1132-1141.
9. Deng X, Li S, Kong F, et al. Long noncoding RNA PiHL regulates p53 protein stability through GRWD1/RPL11/MDM2 axis in colorectal cancer. *Theranostics*. 2020;10:265-280.
10. Lu J, Zhang P-Y, Xie J-W, et al. Circular RNA hsa_circ_0006848 related to ribosomal protein L6 acts as a novel biomarker for early gastric cancer. *Dis Markers*. 2019;2019:3863458.
11. Haupt Y, Maya R, Kazaz A, Oren M. Mdm2 promotes the rapid degradation of p53. *Nature*. 1997;387:296-299.
12. Kubbutat MH, Jones SN, Vousden KH. Regulation of p53 stability by Mdm2. *Nature*. 1997;387:299-303.
13. Dai M-S, Shi D, Jin Y, et al. Regulation of the MDM2-p53 pathway by ribosomal protein L11 involves a post-ubiquitination mechanism. *J Biol Chem*. 2006;281:24304-24313.
14. Bai D, Zhang J, Xiao W, Zheng X. Regulation of the HDM2-p53 pathway by ribosomal protein L6 in response to ribosomal stress. *Nucleic Acids Res*. 2014;42:1799-1811.
15. Deisenroth C, Franklin DA, Zhang Y. The evolution of the ribosomal protein-MDM2-p53 pathway. *Cold Spring Harb Perspect Med*. 2016;6(12):a026138.
16. Ji P, Wang L, Liu J, et al. Knockdown of RPL34 inhibits the proliferation and migration of glioma cells through the inactivation of JAK/STAT3 signaling pathway. *J Cell Biochem*. 2019;120:3259-3267.
17. Dai J, Wei W. Influence of the RPL34 gene on the growth and metastasis of oral squamous cell carcinoma cells. *Arch Oral Biol*. 2017;83:40-46.
18. Fan H, Li J, Jia Y, et al. Silencing of ribosomal protein L34 (RPL34) inhibits the proliferation and invasion of esophageal cancer cells. *Oncol Res*. 2017;25:1061-1068.
19. Luo S, Zhao J, Fowdur M, Wang K, Jiang T, He M. Highly expressed ribosomal protein L34 indicates poor prognosis in osteosarcoma and its knockdown suppresses osteosarcoma proliferation probably through translational control. *Sci Rep*. 2016;6:37690.
20. Liu H, Liang S, Yang XI, et al. RNAi-mediated RPL34 knockdown suppresses the growth of human gastric cancer cells. *Oncol Rep*. 2015;34:2267-2272.
21. Yang S, Cui J, Yang Y, et al. Over-expressed RPL34 promotes malignant proliferation of non-small cell lung cancer cells. *Gene*. 2016;576:421-428.
22. Kun-Peng Z, Chun-Lin Z, Xiao-Long M. Antisense lncRNA FOXF1-AS1 promotes migration and invasion of osteosarcoma cells through the FOXF1/MMP-2/-9 pathway. *Int J Biol Sci*. 2017;13:1180-1191.
23. Villegas VE, Zaphiropoulos PG. Neighboring gene regulation by antisense long non-coding RNAs. *Int J Mol Sci*. 2015;16:3251-3266.
24. Zhang X-D, Huang G-W, Xie Y-H, et al. The interaction of lncRNA EZR-AS1 with SMYD3 maintains overexpression of EZR in ESCC cells. *Nucleic Acids Res*. 2018;46:1793-1809.
25. Tang Z, Li C, Kang B, Gao G, Li C, Zhang Z. GEPIA: a web server for cancer and normal gene expression profiling and interactive analyses. *Nucleic Acids Res*. 2017;45:W98-W102.
26. Ashcroft M, Taya Y, Vousden KH. Stress signals utilize multiple pathways to stabilize p53. *Mol Cell Biol*. 2000;20:3224-3233.
27. Ji L, Fan X, Zhou F, Gu J, Deng X. lncRNA RPL34-AS1 inhibits cell proliferation and invasion while promoting apoptosis by competitively binding miR-3663-3p/RGS4 in papillary thyroid cancer. *J Cell Physiol*. 2020;235(4):3669-3678.
28. Gong Z, Li J, Cang P, Jiang H, Liang J, Hou Y. RPL34-AS1 functions as tumor suppressive lncRNA in esophageal cancer. *Biomed Pharmacother*. 2019;120:109440.
29. Li JH, Liu S, Zhou H, Qu LH, Yang JH. starBase v2.0: decoding miRNA-ceRNA, miRNA-ncRNA and protein-RNA interaction networks from large-scale CLIP-Seq data. *Nucleic Acids Res*. 2014;42:D92-D97.
30. Zhang Y, Guo Y, Zhou X, Wang X, Wang X. Prognosis for different patterns of distant metastases in patients with uterine cervical cancer: a population-based analysis. *J Cancer*. 2020;11:1532-1541.
31. Dong Z, Li S, Wu X, et al. Aberrant hypermethylation-mediated downregulation of antisense lncRNA ZNF667-AS1 and its sense gene ZNF667 correlate with progression and prognosis of esophageal squamous cell carcinoma. *Cell Death Dis*. 2019;10:930.
32. Wang X, Zhang J, Wang Y. Long noncoding RNA GAS5-AS1 suppresses growth and metastasis of cervical cancer by increasing GAS5 stability. *Am J Transl Res*. 2019;11:4909-4921.
33. Yang H, Yang W, Dai W, Ma Y, Zhang G. LINC00667 promotes the proliferation, migration, and pathological angiogenesis in non-small cell lung cancer through stabilizing VEGFA by EIF4A3. *Cell Biol Int*. 2020;44:1671-1680.
34. Bian C, Yuan L, Gai H. A long non-coding RNA LINC01288 facilitates non-small cell lung cancer progression through stabilizing IL-6 mRNA. *Biochem Biophys Res Commun*. 2019;514:443-449.
35. Le Hir H, Séraphin B. EJCs at the heart of translational control. *Cell*. 2008;133:213-216.

SUPPORTING INFORMATION

Additional supporting information may be found online in the Supporting Information section.

How to cite this article: Zhu Y, Ren C, Jiang D, et al. RPL34-AS1–induced RPL34 inhibits cervical cancer cell tumorigenesis via the MDM2-P53 pathway. *Cancer Sci*. 2021;112:1811–1821. https://doi.org/10.1111/cas.14874